

Strain relief in metal heteroepitaxy on face-centered-cubic(100): Cu/Ni(100)

Bert Müller, Lorenz Nedelmann, Björn Fischer, Alexander Fricke, and Klaus Kern
*Institut de Physique Expérimentale, Ecole Polytechnique Fédérale de Lausanne,
CH-1015 Lausanne, Switzerland*

(Received 6 October 1995; accepted 12 February 1996)

Strain relaxation is very important for the fabrication of smooth heteroepitaxial films with abrupt interfaces. At fcc(111) surfaces, strain is very efficiently relieved through the formation of fcc-hcp stackings, which are usually arranged in mesoscopically ordered networks. At fcc(100) surfaces, however, fcc-hcp stacking faults are symmetrically impossible. We report here on a novel mechanism—internal (111) faceting—of strain relief at heterointerfaces with square symmetry. The mechanism has been revealed for thin Cu films on Ni(100) by variable temperature scanning tunneling microscopy. In the first monolayer, monatomic chains of Cu atoms are shifted laterally from the fourfold hollow configuration to the twofold bridge configuration and thereby protrude from the surface layer. The gain in lateral freedom of expansion of the protruding atoms overbalances their lowered binding energy. With each Cu layer added the relaxed stripes grow in width by one atom, forming internal {111} interfaces in the Cu film. In this mode the film grows layerwise up to about 20 monolayers where bulk dislocations are formed through merging stripes.
© 1996 American Vacuum Society.

The preparation of high-quality heteroepitaxial interfaces is an important task in materials science. This is, however, difficult since the lattice mismatch between film and substrate material leads to strain in the film until the film has adopted its bulk geometry through the formation of strain-relieving defects. In the widely accepted classical “Matthews picture” the adlayer is thought to remain locked to the substrate up to a finite critical thickness h_c .¹⁻³ For $h \leq h_c$ the film grows essentially pseudomorphically. For a thickness $h > h_c$ strain is relieved by means of misfit dislocations and associated lattice relaxation. The critical thickness is determined by the elastic constants of both materials and their misfit (m). It can vary from below 1 Å ($|m| > 10\%$) up to 200 Å for small misfits ($|m| \leq 2\%$). This concept is a continuum model, ignoring atomic details of the interface structure. Indeed, it has recently been found to fail in the description of hexagonal close packed metal interfaces.⁴⁻⁶ This failure is related to the particular structure of fcc(111) surfaces with fcc and hcp sites of similar adsorption energy. Strain can easily be accommodated by the formation of fcc-hcp stackings (domain walls). The low energy cost for the formation of misfit dislocations essentially drops h_c to zero or just to the first monolayer.⁴⁻⁶ On the other hand, the fcc-hcp stacking fault mechanism is symmetrically impossible at square interfaces because there are no different sites with similar adsorption energy. For these interfaces many experimental studies have been reported which seem to be in agreement with the predictions of the Matthews picture.⁷ In particular, an Auger electron diffraction study of Cu growth on Ni(100) seemed to provide quantitative support of the continuum model.⁸ Chambers *et al.* interpreted their data in favor of a pseudomorphic growth up to a critical thickness of 8 monolayers (ML), which is indeed the h_c value predicted for this system by the continuum model.

In this article we demonstrate, however, that Cu does not grow pseudomorphically on Ni(100) despite the small lattice

mismatch of only $m = -2.6\%$. Strain-relieving defects are already created in the first monolayer. These defects lead to a nearly perfect layer-by-layer growth up to about 20 ML. But they are also responsible for the drastic change of the growth mode at this coverage, resulting in dislocations of high density. A similar strain-relief scenario has recently been reported for a 2.5 ML film of KCl on NaCl(100).⁹ We thus expect that the *internal (111) faceting* model is of general importance for heterointerfaces with square symmetry.

The experiments were performed with a variable-temperature scanning tunneling microscope (STM) in an ultrahigh vacuum chamber equipped with the usual facilities for sample cleaning, and structural and chemical characterization.¹⁰ The nickel crystal was prepared by Ar⁺ ion sputtering and subsequent annealing to 1200 K. The copper films have been grown by thermal evaporation at a background pressure of better than 5×10^{-10} mbar and deposition rates of 1.5×10^{-3} ML/s. All STM measurements were performed in the constant current mode at 0.2–1.0 V positive or negative tip bias and 0.5–1.5 nA tunneling current. Some of the STM images have been measured in differential mode, which means that the derivative of the lines of constant tunnel current has been recorded (these images represent the surface as it appears when illuminated from the left-hand side).

In Fig. 1 we show a series of STM images characterizing the Cu multilayer growth on Ni(100) at 350 K. In the submonolayer range at coverages of about 0.25 ML (not shown here) long protruding stripes already appear at the islands which have a typical size of 60–80 Å. The stripes protrude by about 0.6 Å, have a width of ~ 6 Å (which is the typical STM-imaging width of a single atom),¹¹ and traverse the entire islands. At a coverage of 1 ML [Fig. 1(a)] the whole surface is covered by a network of stripes. The stripes all have the same width and are all running along $\langle 110 \rangle$ with an equal probability for the two orthogonal domains. This pat-

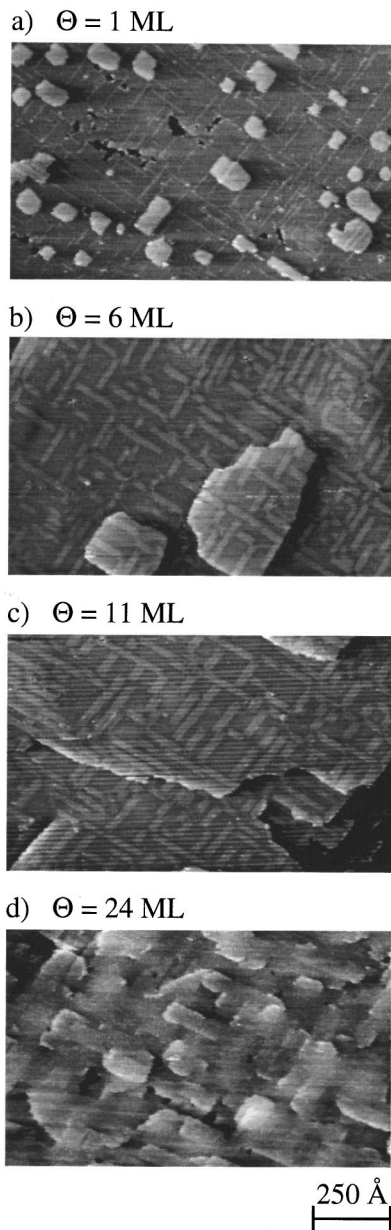


FIG. 1. STM images (a)–(d) characterizing the multilayer growth of Cu on Ni(100). The substrate temperature was 350 K and the deposition rate was 1.5×10^{-3} ML/s.

tern is maintained up to coverages of about 20 ML as shown in Fig. 1. Only the width of the stripes grows linearly with the coverage. The density of stripes and their average length, on the other hand, remain constant in this coverage range. Note that the stripes do not cross each other or coalesce.

In the following we discuss a simple model which accounts for the experimental observations. It is motivated by the fact that the compressive strain at the fcc(100) surface is highest in the close-packed $\langle 110 \rangle$ direction. Therefore, intuitively it could be expected that chains of atoms are squeezed out from the adlayer and create protruding stripes. Due to the square symmetry, these stripes have to form with equal probability in both $\langle 110 \rangle$ directions, perpendicular and parallel to the substrate step edges. The simplest way to generate such

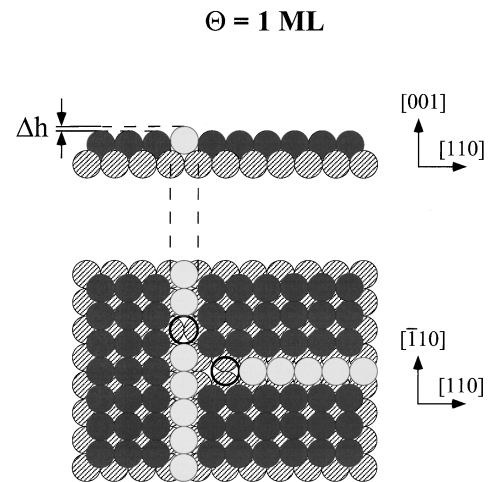


FIG. 2. Model describing the appearance of the stripes in the Cu monolayer on Ni(100). The shaded circles represent the substrate atoms (Ni). The “dark atoms” (Cu) are placed at the fourfold hollow sites in the pseudomorphic geometry. The “light atoms” (Cu) form the stripes and are placed at the twofold bridge sites. One can clearly see the two orthogonal domains of bridge sites which renders crossing of the stripes impossible.

stripes is to shift Cu atoms from their fourfold hollow site to the twofold bridge site (see Fig. 2). Such a bridge-site atom has a reduced number of nearest neighbors in the substrate but gains binding energy in the adlayer. There are two nearest neighbors below and, in addition, four lateral neighbors with a binding length which is only about 10% larger. More important, the protruding atoms gain lateral freedom of expansion and the film can partially relieve its strain. Obviously, this lateral freedom of expansion overbalances the lowered binding energy.

An important experimental observation is the fact that stripes neither cross nor coalesce at all coverages below about 20 ML (see Fig. 1). This behavior is easy to understand in the proposed model. There are two domains of bridge sites on the square fcc(100) surface depending on the direction of the stripes. At their potential junction, two orthogonal stripes are always separated by $1/\sqrt{8}$ of a lattice constant (i.e., $1/2$ the nearest-neighbor distance) rendering crossing impossible (Fig. 2). Coalescence is also unlikely as the distance between two parallel stripes is given by the lattice constant of the Ni substrate and the merging of two stripes would block further transverse relaxation. Therefore, at higher coverages one can find neighboring parallel stripes which have a smaller width than the other stripes at the same image (see Fig. 1, $\Theta=11$ ML). Only at high coverages close to 20 ML, where almost all of the surface is covered by relaxed stripes, do neighboring as well as orthogonal stripes merge and thereby form a high density of bulk dislocations [see Fig. 1(d)].

Figure 3 shows the model for the trilayer film. The height Δh is independent of coverage. Considering the most simple case of a hard sphere model, one obtains $\Delta h=0.4$ Å for the growth of Cu on Ni. The width D depends on the coverage, i.e., for 1 ML the stripes are exactly one atom wide, for 2 ML they are two atoms wide, and so on. While the atoms, situated at the hollow sites (dark colored atoms), grow essen-

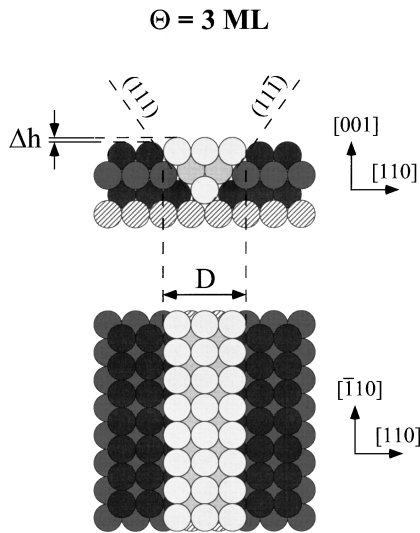


FIG. 3. The internal (111) faceting model for Cu/Ni(100) at a coverage of 3 ML. The shaded circles represent the substrate atoms (Ni). The “dark atoms” (Cu) are placed at the fourfold hollow sites in the pseudomorphic geometry. The “light atoms” (Cu) form the stripes and are placed at the twofold bridge sites in the first layer. As indicated, {111} facets are formed along the stripes.

tially pseudomorphically, the stripe atoms (light colored) can relieve strain at least perpendicular to the stripes.¹² In our model the density of the stripes and their length distribution is determined by the monolayer configuration. The subsequent growth stabilizes the pattern of stripes by the formation of internal {111} facets along the stripes. This is energetically favorable because the strain relaxation takes place by the formation of the highly stable close-packed {111} facets.

The internal (111) faceting model¹³ is in quantitative agreement with our experimental observations. The first graph of Fig. 4 shows clearly that the height of the stripes is constant for all coverages. The height Δh was found to be $(0.6 \pm 0.1) \text{ \AA}$, which is in fair agreement with the simple hard sphere model ($\Delta h = 0.4 \text{ \AA}$). The linear dependency of the width of the stripes on the coverage is demonstrated in the second graph of Fig. 4. The horizontal lines indicate the stepwise growth of the width D as expected from our model. It should be mentioned that we have plotted corrected stripe widths in Fig. 4, taking into account the finite imaging width of the STM tip.¹¹

Above monolayer coverage the mean length of the stripes $\langle s \rangle$ remains constant, $(65 \pm 5) \text{ \AA}$, independent of film thickness. This value corresponds to (26 ± 2) atoms. The density of stripes ρ is likewise constant, $(8.0 \pm 1.4) \times 10^{-4}$ per substrate atom, for coverages between 1 and 20 ML. The quantitative analysis of the images reveals that the density of the stripes as well as the length distribution are determined by the monolayer configuration. In Fig. 5 we plot the measured length distribution of the monolayer Cu film. The distribution of stripe lengths can best be described by the following exponential law (see the full line in Fig. 5):

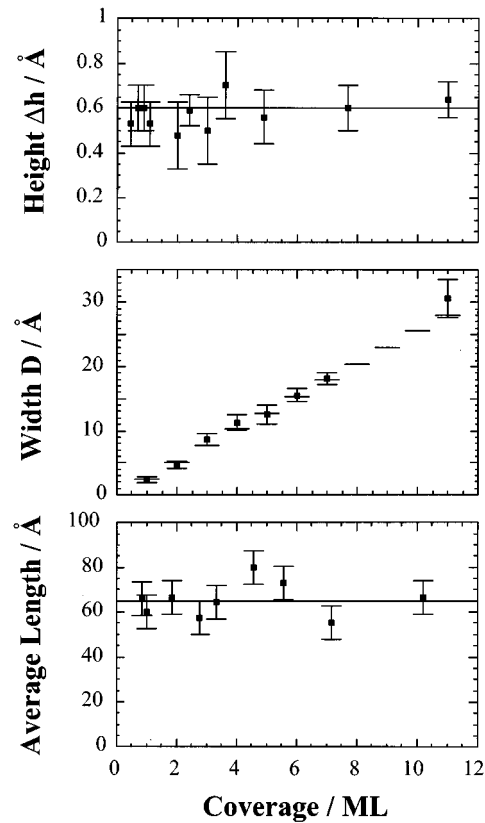


FIG. 4. Quantitative analysis of the pattern of the stripes observed on Cu/Ni(100). Plotted are the height Δh (a), the width D (b), and the average length of the stripes (c), all quantities as a function of Cu coverage.

$$N_s(s) = \frac{\rho}{\langle s \rangle} \exp\left(-\frac{s - s_{\min}}{\langle s \rangle}\right),$$

where ρ is the density of the stripes and $\langle s \rangle$ is their average length. For the minimum stripe length s_{\min} we have chosen 10 atoms according to the experimental data in Fig. 5. Stripes of less than 8 atoms have not been observed. These

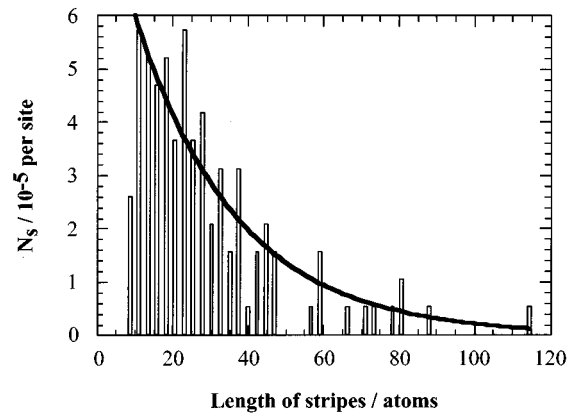


FIG. 5. Length distribution of the stripes (raw data). The solid line represents the exponential distribution, whereby an average length of 27 atoms, a minimal length of 10 atoms, and a density of the stripes of 6.8×10^{-4} per lattice site are assumed.

stripes seem to be energetically unstable. From the energetic point of view, longer stripes are more stable. The length of the stripes is, however, limited by their geometric arrangement since the stripes occur with equal probability in the $[\bar{1}10]$ and $[110]$ directions and the crossing of orthogonal stripes is impossible. The exponential distribution function seems to have “universal” character. The distribution does not vary markedly with deposition rate (1.34 or 2.89×10^{-3} ML/s), substrate temperature (between 200 and 400 K), or coverage (1 – 17 ML). Even the annealing of the film up to 1000 K does not change the distribution or the average length. This behavior is also valid for the density of the stripes. Therefore we believe that the formation of the stripes is essentially determined by the strain and not by the growth kinetics.

The growth of thin Cu films on Ni(100) was also studied by Chambers *et al.*⁸ by means of Auger electron diffraction (AED). The ratio of the in-plane to vertical lattice constant (transverse lattice expansion) was measured, which is directly related to the strain of the film. The authors compared their data with the predictions of the continuum model of Matthews and Crawford.² The continuum model predicts a critical thickness of $h_c = 14.8 \text{ \AA} \approx 8$ ML. Up to this thickness, Cu should grow pseudomorphically. Only at coverages above 8 ML should the film relax its strain spontaneously by the formation of bulk dislocations. Chambers *et al.* interpreted their experimental data as confirmation of the continuum model. However, the internal (111) faceting model describes the almost linear behavior of the transverse lattice expansion on the coverage much better. Contrary to the classical continuum model, our study shows that the film relieves its strain gradually in a layer-by-layer fashion. A detailed discussion of the quantitative comparison between our internal faceting model and the AED data is given in Ref. 14.

The internal faceting mechanism should be applicable to interfaces with noncovalent bonding, i.e., metals, ionic- or van der Waals-bonded crystals. The directional bonding at semiconductor interfaces usually results in an open and more complex structure. For example, the V-shaped defects in epitaxial Ge layers grown on Si(001) in the presence of As observed by LeGoues, Copel, and Tromp¹⁵ using high-resolution transmission electron microscopy are also strain induced and bear similarities to the defect structures based on the internal faceting model. The structure of the V defects is, however, fundamentally different due to the covalent nature of the Ge bonding. Moreover, STM measurements of Ge

growth on As-terminated Si(100) by Jusko *et al.*¹⁶ do not provide any evidence for protrusion stripes or the characteristic layer-by-layer variation of the defect structures, as seen in the case of the internal faceting mechanism.

Finally, we want to point out that the stripe pattern at the surface substantially influences the nucleation and thus the growth mode of the Cu film. The protruding stripes act as diffusion barriers and heterogeneous nucleation centers. This is evident in Fig. 1. The islands nucleate preferentially at stripes and have a rectangular shape. In particular, the enhanced nucleation density is responsible for the almost perfect layer-by-layer growth up to 20 ML.¹⁷

Acknowledgements: Three of the authors (B.M., A.F., and L.N.) gratefully acknowledge support of the Alexander von Humboldt-Stiftung and of the Deutscher Akademischer Austauschdienst, respectively.

¹F. C. Frank and J. H. van der Merwe, Proc. R. Soc. London Ser. A **198**, 205 (1949).

²J. W. Matthews and J. L. Crawford, Thin Solid Films **5**, 178 (1970).

³R. Bruinsma and A. Zangwill, J. Phys. **47**, 2055 (1986).

⁴H. Brune, H. Röder, C. Boragno, and K. Kern, Phys. Rev. B **49**, 2997 (1994).

⁵C. Günther, J. Vrijmoeth, R. Q. Hwang, and R. J. Behm, Phys. Rev. Lett. **74**, 754 (1995).

⁶J. A. Meyer, P. Schmid, and R. J. Behm, Phys. Rev. Lett. **74**, 3864 (1995).

⁷*Epitaxial Growth*, edited by J. A. Matthews (Academic, New York, 1975).

⁸S. A. Chambers, H. W. Chen, I. M. Vitomirov, S. B. Anderson, and J. H. Weaver, Phys. Rev. B **33**, 8810 (1986).

⁹M. Henzler, C. Homann, U. Malaske, and J. Wollschläger, Phys. Rev. B **52**, 17 060 (1995).

¹⁰H. Brune, H. Röder, C. Boragno, and K. Kern, Phys. Rev. Lett. **73**, 1955 (1994); Appl. Phys. A **60**, 167 (1995).

¹¹Monatomic Cu chains are usually imaged with a width of ~ 5 – 8 Å; J. P. Bucher, E. Hahn, P. Fernandez, C. Massobrio, and K. Kern, Europhys. Lett. **27**, 473 (1994).

¹²It cannot be excluded, and might even be likely that the hollow-site atoms are not perfectly pseudomorphic but partially relaxed, particularly close to the stripe boundary.

¹³The internal faceting model can equivalently be described as an inclined stacking fault mechanism because each close-packed facet plane corresponds to an inclined stacking fault along (111). In this terminology the pairing of stacking faults with opposite inclination assures the planar growth of the (100) surface.

¹⁴B. Müller, L. Nedelmann, B. Fischer, A. Fricke, and K. Kern, Phys. Rev. Lett. **76**, 2358 (1996).

¹⁵F. K. LeGoues, M. Copel, and R. Tromp, Phys. Rev. Lett. **63**, 1826 (1989).

¹⁶O. Jusko, U. Köhler, G. J. Pietsch, B. Müller, and M. Henzler, Appl. Phys. A **54**, 265 (1992).

¹⁷G. Rosenfeld, R. Servanty, C. Teichert, B. Poelsema, and G. Comsa, Phys. Rev. Lett. **71**, 895 (1993).